Prabha Materials Science Letters
Vol. 5, No. 2, 432-445, 2026
https://doi.org/10.33889/PMSL.2026.5.2.024

Characterization of Weld Deposits of AISI SS 316L on AISI 1020 Steels by Robotic HW-GTAW Process

Ishank
Department of Mechanical Engineering,
Sant Longowal Institute of Engineering and Technology, Longowal, Sangrur, Punjab, India.
Corresponding author: pme2206_ishank@sliet.ac.in

Jaspal Singh Gill
Department of Mechanical Engineering,
Sant Longowal Institute of Engineering and Technology, Longowal, Sangrur, Punjab, India.
E-mail: jsgill@sliet.ac.in

Mohd. Majid
Department of Mechanical Engineering,
Sant Longowal Institute of Engineering and Technology, Longowal, Sangrur, Punjab, India.
E-mail: mohdmajid@sliet.ac.in

(Received on April 15, 2026; Revised on June 11, 2026 & July 3, 2026; Accepted on July 13, 2026)

Abstract
American Iron and Steel Institute 316L weld overlays were deposited on AISI 1020 steel using the hot-wire GTAW process with a robotic setup. The addition of hot filler wire in the GTAW process can be successfully employed to achieve a smooth weld bead appearance and improved deposition characteristics. Heating of the filler wire has been based on resistive heating, where the equipment supplies a heating current ranging from 40 A to 60 A, thereby raising the temperature to approximately 200°C. This study aims to analyze the efficacy of weld-clad deposits and the effects of welding parameters on their characterization and metallurgical behavior. A comparative study was conducted between conventional GTAW and hot wire addition GTAW (HW-GTAW), utilizing robotic manipulation of the welding torch to lay down the deposit in a weaving motion of 10 mm on both sides. Single-pass clad-bead experiments were conducted to characterize the deposition. The bead profile studies of these experiments were performed, and the percentage dilution of the filler for each experiment was analyzed. Minimum dilution of 15.96 % has been observed at 185 A of welding current and 55 A of hot wire current. Also, under the same welding conditions, microhardness was found to be maximum, which is around 450 HV. Microstructural observations reveal a finer and more uniform grain structure, which aligns with the obtained microhardness values.

Keywords- Hot wire GTAW (HW-GTAW), Robotic weaving, Deposition, Dilution, Microhardness, Microstructure.

1. Introduction
Engineering components subjected to diverse types of wear, such as corrosive, erosive, impact, abrasive, etc., lead to service, functional, financial, and other losses that need to be addressed. So, continuous efforts are made to inhibit the loss due to wear, and components are prepared to withstand the wear conditions with greater endurance. Surface engineers use various weld overlays or cladding techniques to achieve the upgradation of surface quality and strength of these components. In this context, the demand for clad components is steadily rising across various industries such as mining, agriculture, power generation, naval, chemical, etc. Also, tool manufacturers are employing different cladding techniques to produce tools such as jaws, dies, rollers, etc., that demand enhanced hardness, wear resistance, and compressive strength (Munro & Chen, 2020).

Weld cladding is a procedure used for improving surfaces with desired properties by applying a layer of approximately 3 mm of filler on the substrate or base metals, using any of the arc welding processes. (GTAW) Gas tungsten arc welding (hot wire and cold wire), (GMAW) Gas metal arc welding, (SMAW) Shielded metal arc welding, (SAW) Submerged arc welding, (FCAW) Flux cored arc welding, (ESSC) Electroslag strip welding processes are widely used for cladding jobs (Aslam & Sahoo, 2022).

Despite its fair process capabilities and advantages like easy arc maintenance and better controls, the GTAW process gained popularity incredibly early. The need to get better results from this process led to the development of variants of this process, like Pulsed GTAW, Hot wire GTAW, electromagnetic vibration-assisted GTAW, ultrasound GTAW, keyhole GTAW, and activated GTAW (Pavan et al., 2023). Hot filler addition in the conventional GTAW process is used for the present research. Preheating of filler wire can be achieved by passing current through it from an additional power source, which induces resistive heating. In the conventional GTAW process, filler wire takes heat from the molten pool and gets deposited on the substrate. On the other hand, in hot wire GTAW, preheating of the filler wire to approximately 200 degrees is done through resistive heating before it enters the weld pool, which reduces the amount of heat required from the molten pool. As a result, a lower welding current can be used, leading to reduced heat input to the substrate. This idea was developed in the patent titled 'Consumable Electrode Arcless Electric Working' applied by Manz (1964), & Hori et al. (2004). The quality of the clad bead operated on GTAW is mainly influenced by input parameters such as welding current, arc voltage, and travel speed (Raj & Gill, 2023; Shakya et al., 2024). This type of preheating is conducted externally with an auxiliary power source before being fed into the primary arc zone (Gill & Majid, 2023). The integration of robotic weaving with the hot wire GTAW process aligns it with the growing digitization demands and advancements of intelligent manufacturing systems. This approach not only ensures a high level of automation but also facilitates the economical production of complex component geometries. The set-up that includes weaving by a robotic arm and preheating by an auxiliary power source improves weld bead quality, lowers dilution rates, and incredibly reduces the number of passes (Chen et al., 2014).

The resistive preheating of filler wire through an additional power source in the hot-wire GTAW process, the hot wire current (typically 40-80 A for 1-1.5 diameter wire) controls the thermal dynamics through Joule resistive heating of the filler wire before it enters the weld pool. Preheating of filler reduces the overall heat input in the weld pool, which results in minimizing the penetration depth, increasing the weld width and reinforcement and decreasing the area of fusion due to reduced arc penetration.

On increasing the preheating temperature periodically, the heat input and metallurgical changes are discussed in the following table (Padmanaban et al., 2017; Aloraier et al., 2025).

Table 1. Metallurgical changes according to the preheating temperature increment.

Hot wire current range	Thermal effects on the process
40-60 A	Preheating reaches 200-280 °C. This modest preheating reduces the arc energy needed for melting, but is limited by pool fluidity.
60-80 A	Wire tip reaches to 360-450 °C, which is close to the melting point of the filler wire and reduces the arc heat requirement by 15-20 %.
80-100 A	Wire approaches the melting point before entering the weld pool, which requires a higher wire feed rate, causing a magnetic arc blow problem in which the arc is deflecting to either side (towards the filler wire or away from it).

Dilution during the cladding operation is the factor that decides the richness of the filler chemistry of the clad deposit. More dilution depicts that another layer of the filler is required to get a closer composition to that of the filler material. Dilution control has, therefore, remained a topic of interest to save resources (Gill & Shahi, 2016).

Many researchers have conducted investigations to select the welding parameters to achieve desired weld penetration and bead characteristics in welding as well as cladding operations. The latest literature aspects and technological advancements in hot wire GTAW provide help to modern manufacturing in developing defect-free welding structures. During the fabrication of steam generators, Pai et al. deliberated on issues related to poor impact strength and inadequate deposition, leading to the application of preheating the filler wire during the process. Hot filler wire addition with the conventional GTAW process overcomes the flaws, as hot wire GTAW resulted in higher deposition rates with adequate impact strength (Pai et al., 2014). The concept of hot wire was also utilized in the fabrication of steel bridges by Tsuyama et al. (2014) where the SAW (submerged arc welding) process was used. To enhance the efficiency of weld production in steel bridges, preheated filler wire was introduced into the trailing edge of the weld pool, positioned behind the guiding electrode; as a result, heat input was suppressed to a great extent, and weld deposition was increased (Tsuyama et al., 2014). Improved microstructure that consists of dendrites, equiaxial and cellular crystals, was observed in an experiment by Wang et al. (2022), in which hot wire GTAW was assisted in wire arc additive manufacturing (WAAM) during the fabrication of Inconel 625 thin-wall structure. It was a great idea to assist hot wire GTAW in WAAM for getting high deposition efficiency and the wide use of nickel-based alloy Inconel in aerospace, petrochemical, and marine engineering (Wang et al., 2022). Reduced heat input obtained in the hot wire GTAW process resulted in higher deposition, improved microstructure, and higher strength properties in an optimized experimentation of AISI 316 N joining by Neelamegam et al. (2024). In this research, hot wire current, wire feed, welding speed, and welding current were input variables, and weld cross-sectional area, depth of penetration, and bead width were response measures. The experimentation concluded that the lower heat input reduces the number of attempts to attain the specific deposition, weld joints were free from defects, and better tensile properties (Neelamegam et al., 2024). The combination of welding current with hot wire current highly influenced weld bead profiles, dilution, microhardness, and various strength properties. Concerning this, experimentation by Sashank et al. (2024) investigated the welding characteristics of welded joints of two dissimilar metals by the hot wire GTAW process. Defect-free welded structures were obtained at higher values of welding current, moderate values of wire feed rate, and constant values of hot wire current with significantly improved values of tensile strength and microhardness (Sashank et al., 2024). Hot wire addition in GTAW requires a heating source for preheating the filler wire. The method of heating the filler wire has a great impact on metallurgical properties. Related to this aspect, a comparative study by Cao et al. (2018) was conducted between conventional GTAW and hot filler addition GTAW that focused on wire heating methods, viz., conduction heating, resistance heating, and arc heating. It was observed that hot wire GTAW by conduction heating was far superior, but complex to obtain, as compared to the other heating methods. The conduction heating method is non-magnetic, which eliminates the magnetic arc blow problem of resistance heating. Also, fine-grained microstructure, superior weld bead appearance, and better welding speed were obtained by conduction heating (Cao et al., 2018).

2. Stringer and Weaving Techniques in Welding and Cladding Operations

To overcome the deficient performance of the procedure, to optimize weld width, and to reduce the number of passes, the weaving technique was introduced in the cladding operation (Zhao et al., 2024). The cladding of parts and components using the weaving technique results in improved weld bead quality, lowered dilution rates, and widened weld bead width (Sandhu & Shahi, 2016). The main functional difference occurs when the travel motion of the torch shifts from stringer to weaving: the bead width is typically 2-4 mm for stringer motion and can be enhanced to 10-12 mm when we apply robotic weaving. Along with that, the heat input is applied over a wider area in the weaving motion, whereas it is concentrated in a narrow zone during the stringer motion. Penetration depth also gets shallower and more uniform across the width due to coverage of a large space, and as a result, dilution is decreased (Costa et al., 2024).

A comparative study by Pravin et al. explored the movement of the electrode in the stringer position and weaving motion with single-layer Inconel 625 clads. The electrode weaving technique produced clad beads with greater width, higher reinforcement, and lower dilution with base metal, offering at low welding currents (Kumar & Shanmugam, 2020). Carvalho et al. (2023) explored the outcomes of different parameters in wall-building operations, incorporating wire arc additive manufacturing (WAAM) of Inconel 625 on low-carbon steel. Bead penetration, bead geometry, dilution, and weld quality were controlled and tailored by optimized parameters such as travel angle, contact-tip-to-work distance (CTWD), travel speed, and heat input. Experimental findings showed that arc power had a direct influence on weld penetration and iron content, with both increasing proportionally (Carvalho et al., 2023). Hot wire GTAW combined with wire arc additive manufacturing suppressed the heat input and refined the columnar grains in a study of manufacturing titanium alloy, as reported by Li et al. (2019). The mechanical properties followed the grain changes, and the anisotropy disappeared when hot wire GTAW was used (Li et al., 2019).

However, robotic weaving has been widely explored in the WAAM procedure to create wall structures, but its application in arc weld cladding is notably limited, with relatively few studies that have investigated its potential in this area.

In the present study, robotic weaving is employed with conventional GTAW and hot wire GTAW processes in depositing AISI 316 L filler on AISI 1020 steel plates. Dilution, bead width, microstructures, and microhardness in the beads are closely monitored with hot wire current, welding current, wire feed, and welding speed.

3. Material Selection (AISI 316 L)

Stainless steel (SS) is the general term applied to a group of corrosion-resistant materials containing a minimum of 10-11 % of chromium with or without low carbon (L) content. Austenitic stainless steels like SS 301, 303, 304, 309, 316 and 316L were developed with increased amount of Cr (13-18 %) and Ni (9-10 %), Mo (2-2.5 %) with lowered carbon content to 0.01 % to get it more corrosion resistant as compared to martensitic stainless steel such as 416, 420, 431 (12-14 % Cr & 0.08-0.15 C) and ferritic steels SS 430 F, 409, 434 (14-15 Cr and Ni, Mo, Ti and Nb can be added). AISI 316 L is a chromium-nickel-molybdenum stainless steel with an austenitic phase that is widely employed as a cladding and coating agent to prevent corrosive attacks on the surface. AISI 316 L has 14-18 % chromium, which generates a thin passive layer on the surface of steel to prevent any further corrosion. The low carbon percentage (<0.03) prevents the tendency of hot cracking of AISI 316 L. The extra low carbon helps to avoid the formation of chromium-rich carbides during welding (Malhotra et al., 2021; Kumar et al., 2024). Intergranular corrosion, sensitisation, and the need for post-weld heat treatment in steel components are prevented by lowering the carbon content in a given alloy. Using AISI 316L filler wire having 0.015 wt% of Carbon content with (16–18 wt% Chromium, and 1–2 wt% Molybdenum) for cladding significantly enhances corrosion resistance by suppressing chromium carbide precipitation and associated chromium depletion at grain boundaries; concurrently, molybdenum promotes repair and stability of the passive film, thereby improving resistance to pitting and crevice corrosion.

AISI 316 L is widely used in applications that demand greater corrosion resistance and better strength at high temperatures. Typical uses include exhaust manifolds, furnace parts, jet engines, pumps, heat exchangers, surgical instruments, textiles, and seashore equipment (de Oliveira et al., 2023). The chemical composition by weight percentage is available in **Table 2**.

Table 2. Chemical composition (wt.%) of AISI 316 L filler material.

Grade	C	Si	S	P	Mn	Ni	Cr	Mo	Fe
AISI 316 L	0.015	0.4	0.02	0.02	1.4	10	17.8	2.3	Balance

4. Experimental Procedures and Setup

GTAW set up with a hot wire, as shown in **Figures 1** and **2**, is used for the present research. For the weaving operation, the secure placement of the GTAW torch on the robotic arm is fabricated and available at the welding metallurgy laboratory, SLIET Longowal, Punjab. A schematic view of the whole set-up is shown in **Figure 3**.

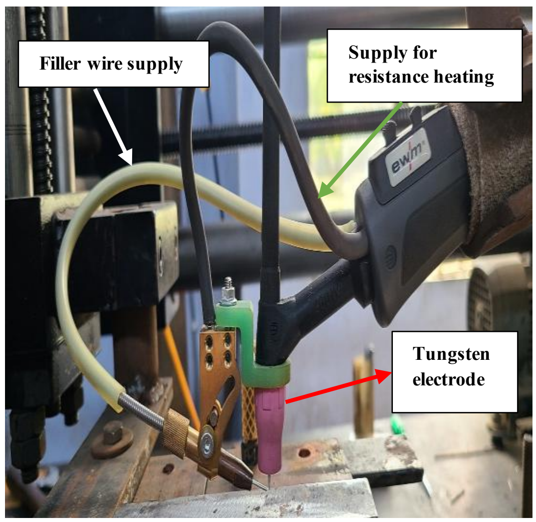

Figure 1. Hot filler wire addition to the GTAW torch.

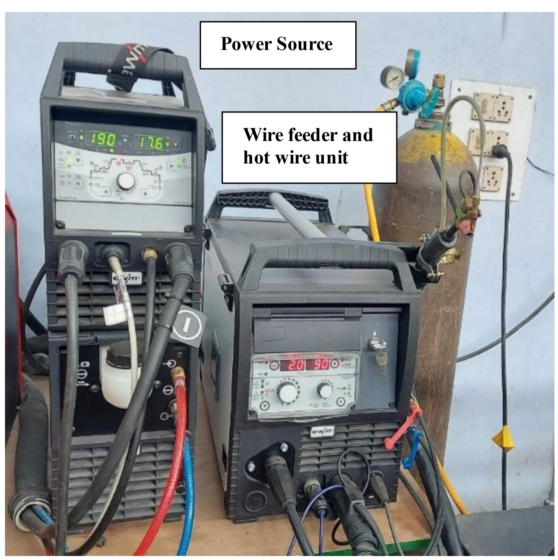

Figure 2. Wire feeding and hot wire unit.

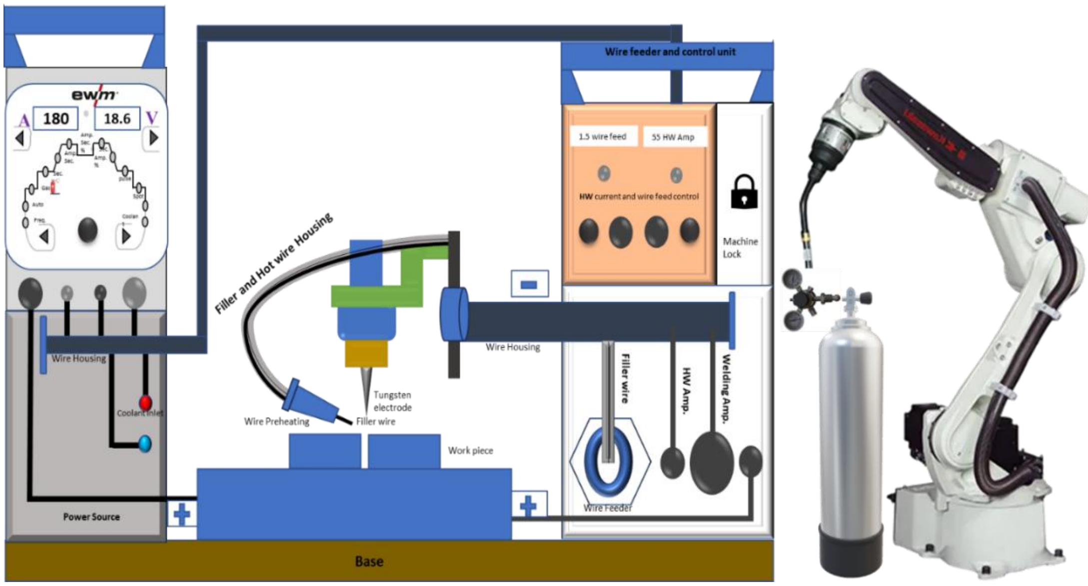

Figure 3. Schematic of hot-wire GTAW setup.

Experiments using Bead on plate method were executed for stringer and weaving beads, keeping gas flow rate at 16 L/min, welding speed 0.08 m/min, robotic frequency 0.5 Hz, robotic weaving width 10 mm, nozzle to plate distance (NPD) at 3mm, wire feed rate at 1, 1.2, 1.5 and 2 m/min and four levels of hot wire currents 0, 40, 50, 55 and 60 A with welding current operated on 180, 185, 190, 195 and 200 A. The experiments were conducted in three stages, and the results of the previous stage guided the next stage of experiments. The bead profile and dilution percentage were calculated using a stereo zoom microscope and ImageJ software. Etching was performed using a Carpenter solution ($FeCl_3$, $CuCl_2$, HCl, HNO_3, and ethanol).

5. Results and Discussion

5.1 Macrostructures

In the first stage of the experiment, stringer beads AISI 316 L were made on an AISI 1020 plate using conventional GTAW and hot wire GTAW processes to get wider bead widths and lower penetration. After conducting the first stage of the experiment, it was observed that with the increase of hot wire current, bead width increases and dilution decreases. However, it has been noticed that higher values of wire feed with increasing hot wire current disrupt the bead profile as the weld reinforcement form factor (WRFF) goes less than 1, which is undesirable for cladding purposes. As clearly shown in **Figure 4** and **Table 3**, the developed beads E, F, G, H, and I have WRFF less than 1. Based on the first stage of the experimentation performed, a range of working parameters has been selected for the next stage of experimentation using robotic weaving.

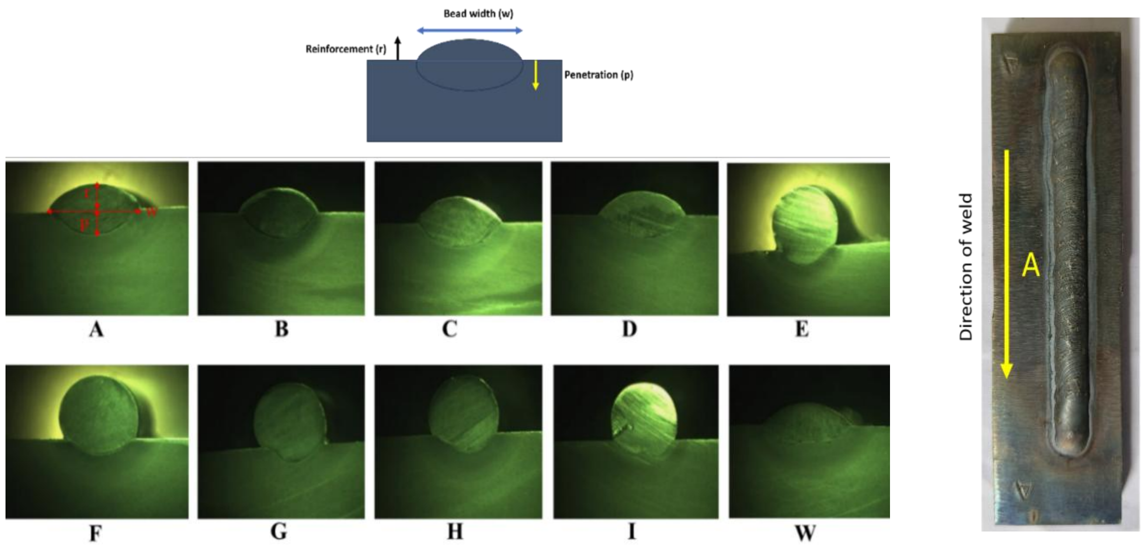

Figure 4. (First set) Macroscopic images of stringer beads.

Table 3. (First set) Observations of weld bead profiles of clad beads with stringer technique.

Sr. No.	Welding current (A)	Hot wire current (A)	Wire feed (m/min)	Welding speed (m/min)	(w) Bead width (mm)	(p) Pen. (mm)	(r) Rein. (mm)	A_P (mm^2)	A_R (mm^2)	Dilution = $(100)(A_P/(A_P+A_R))$ in percentage
W	180	0	1	0.08	6.25	4.20	1.8	18.6	18.89	49.61
A	180	40	1	0.08	6.92	4.08	1.93	18.32	18.96	49.14
B	180	50	1	0.08	7.64	3.76	2.11	18.02	19.13	48.50
C	180	60	1	0.08	6.47	4.41	1.63	18.83	18.72	50.14
D	180	70	1	0.08	6.11	4.70	1.37	18.97	18.62	50.46
I	180	0	2.0	0.08	4.95	1.2	5.08	4.77	**24.99**	**16.02**
E	180	40	2.0	0.08	4.57	0.98	4.84	4.79	**26.73**	**15.19**
F	180	50	2.0	0.08	4.27	0.73	4.94	4.44	**29.22**	**13.19**
G	180	60	2.0	0.08	4.1	0.79	4.86	4.44	**29.63**	**13.03**
H	180	70	2.0	0.08	4.26	0.94	4.67	4.96	**26.5**	**15.76**

In the next stage of experimentation, robotic weaving was employed with a frequency of 0.5 Hz with a 10 mm weaving width. It was observed that with a wire feed increase of 0.2 m/min from the lower value of the first stage, the bead width approximately doubled, and dilution significantly reduced relative to the initial stage. The results show that dilution continuously decreases with an increase in the hot wire current. It is also worth mentioning that as the hot wire current is increased beyond 60 A, the dilution shows a reverse trend with different wire feed values. Keeping the same welding speed when we constantly increase the hot wire current, it will increase the arc pressure on the substrate. Due to an excessive amount of molten metal being supplied into the weld pool, the heat input increases, which lifts the penetration depth, and dilution is increased. Therefore, a hot wire current of less than 60 A, i.e., 55 A, with a wire feed increment (0.3 to 0.5 m/min) was selected for the next stage of the experimentation. Macroscopic images and observations are shown in **Figure 5** and **Table 4**.

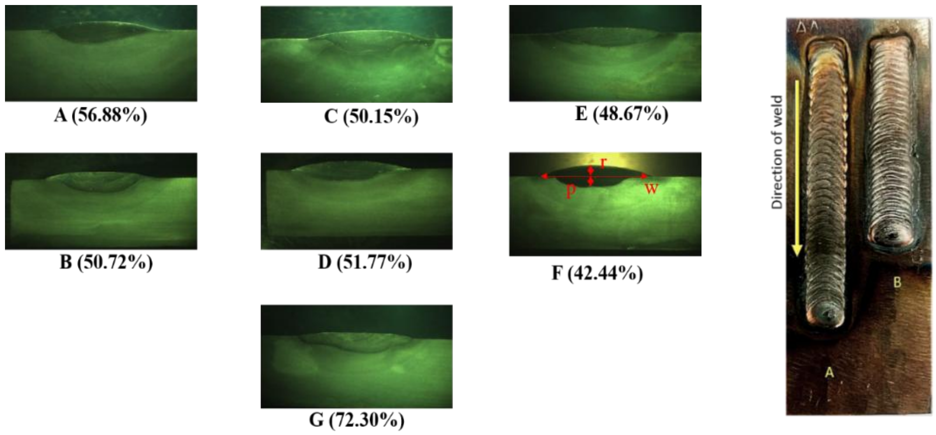

Figure 5. (Second set) Macroscopic images of weaving beads.

Table 4. (Second set) Observations of weld bead profiles of clad beads with weaving technique.

Sr. No.	Welding current (A)	Hot wire current (A)	Wire feed (m/min)	Welding speed (m/min)	(w) Bead width (mm)	(p) Pen. (mm)	(r) Rein. (mm)	A_P (mm²)	A_R (mm²)	Dilution = $(100)(A_P/(A_P+A_R))$ in percentage
A	180	0	1	0.08	8.02	3.56	1.65	15.75	11.94	56.88
B	180	40	1	0.08	9.37	2.05	1.77	13.01	12.64	50.72
C	180	50	1	0.08	9.81	1.98	1.81	12.97	12.89	50.15
D	180	60	1	0.08	9.62	2.03	1.28	13.11	12.21	51.77
E	180	40	1.2	0.08	10.86	1.97	1.89	12.63	13.32	48.67
F	180	50	1.2	0.08	10.90	1.68	1.96	10.31	13.98	42.44
G	180	60	1.2	0.08	10.02	2.38	0.53	18.14	6.95	72.30

The range of welding parameters and macroscopic images for the final stage of the experimentation is mentioned in **Table 5** and **Figure 6**. At this stage, a minimum dilution of 15.96 % was recorded, while the weld width reached a maximum of 13.8 mm at a wire feed rate of 2 m/min with the robotic weaving technique. This condition is referred to as F1.

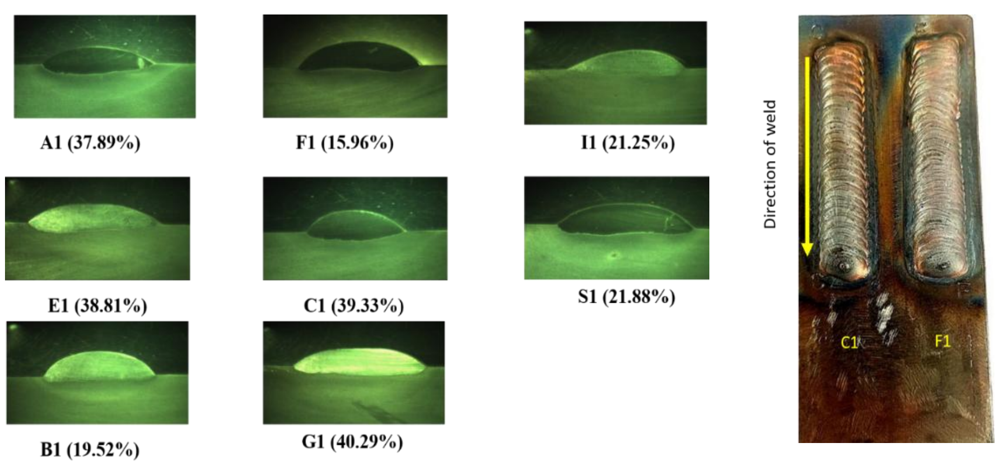

Figure 6. (Third set) Macroscopic images of weaving beads.

Table 5. (Third set) Observations of weld bead profiles of clad beads with weaving technique.

Sr. No.	Welding current (A)	Hot wire current (A)	Wire feed (m/min)	Welding speed (m/min)	(w) Bead width (mm)	(p) Pen. (mm)	(r) Rein. (mm)	A_P (mm^2)	A_R (mm^2)	Dilution = $(100)(A_P/(A_P+A_R))$ in percentage
A1	185	55	1.5	0.08	11.7	1.23	2.7	14.21	23.29	37.89
E1	190	55	1.5	0.08	11.8	1.46	2.5	14.71	23.19	38.81
C1	195	55	1.5	0.08	11.01	1.58	2.33	14.90	22.98	39.33
G1	200	55	1.5	0.08	10.80	2.08	1.93	15.21	22.54	40.29
F1	**185**	**55**	**2**	**0.08**	**13.8**	**0.70**	**3.91**	**7.2**	**37.9**	**15.96**
B1	190	55	2	0.08	12.94	0.79	3.82	8.53	35.17	19.52
I1	195	55	2	0.08	12.01	1.11	3.09	9.06	33.56	21.25
S1	200	55	2	0.08	11.91	1.36	2.98	9.27	33.08	21.88

5.2 Microstructures

The microstructure examination was carried out on the selected samples and is presented in **Figures 7**, **8** and **9**. The figure indicates that all the samples have a similar honeycomb structure with fine equiaxed, short-length, and medium-length columnar grains, which contribute to superior mechanical properties (Rashid et al., 2017). Further investigation reveals that the solidification patterns of all the samples differ from each other, as evident from the Scanning Electron Microscopy (SEM) images. The samples B1 and C1 have a bit of random solidification due to high dilution, as compared to sample F1, indicating the mixing of base metal elements in them. The SEM image also shows that the grain boundaries were not fully developed during solidification in these samples. On the other hand, the sample F1 provided smooth and symmetric solidification, which is due to low dilution and less mixing of base metal particles, and the grain boundaries were fully developed. It is also observed that the orientation of solidification was symmetric inside the grain boundaries of sample F1. The primary morphological differences observed in the SEM analysis of samples at low and high dilution levels are associated with variations in solidification patterns and the presence of fine and coarse dendritic structures. The sample exhibiting higher dilution is characterised by a higher welding current, which increases the heat input, weld pool penetration, and the extent of dilution. The elevated heat input reduces the cooling rate during solidification, thereby promoting grain growth and resulting in the development of coarser dendritic microstructures.

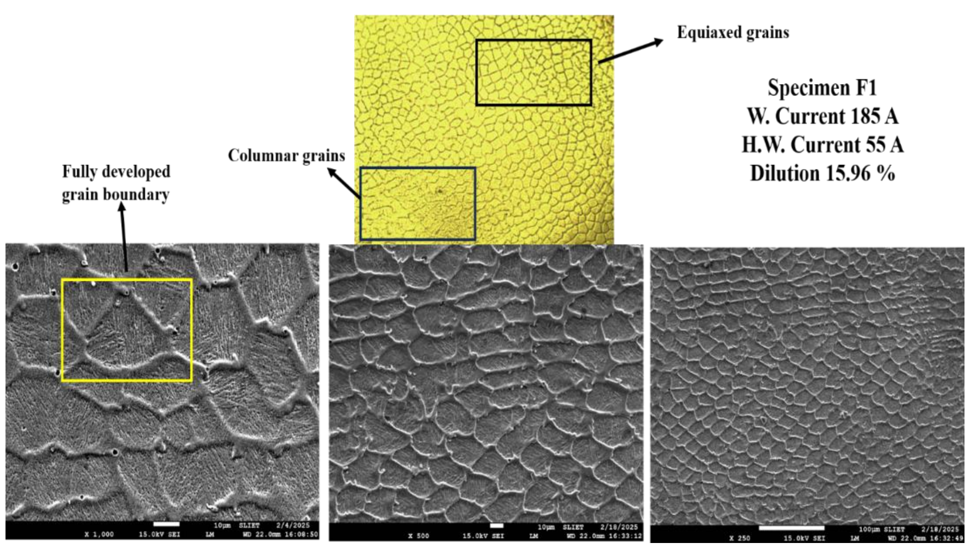

Figure 7. Microstructure and SEM images of clad beads (sample F1).

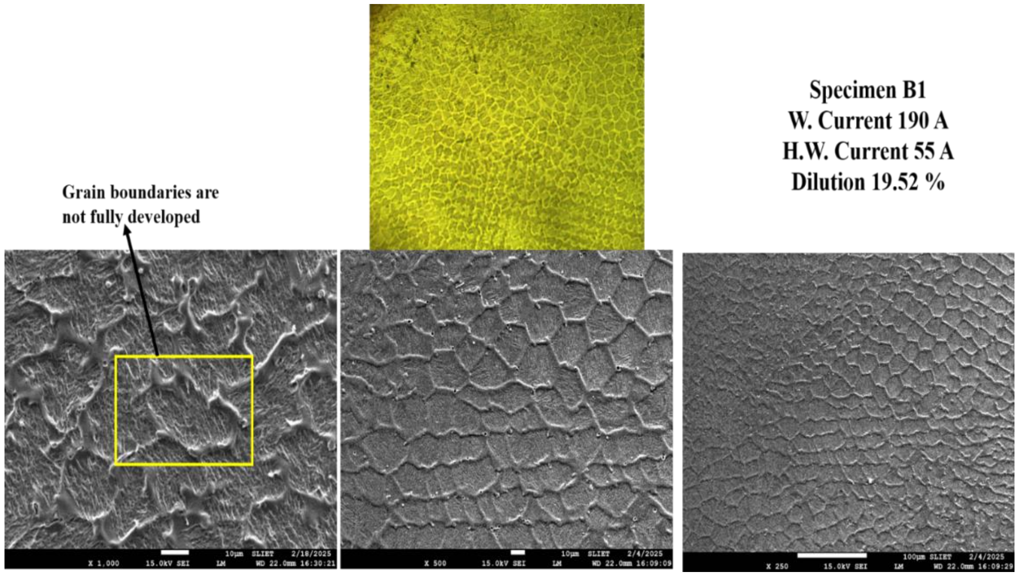

Figure 8. Microstructure and SEM images of clad beads (sample B1).

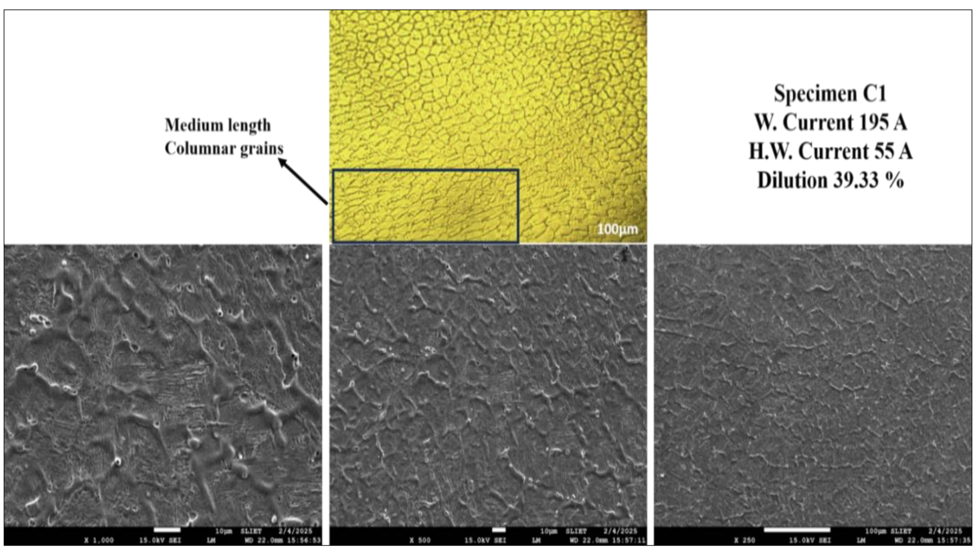

Figure 9. Microstructure and SEM images of clad beads (sample C1).

5.3 Microhardness

The microhardness variation pattern of the weld beads is illustrated in **Figure 10**, developed by robotic weaving with different values of hot wire current, as discussed in **Table 5**. From the figure, it can be seen that microhardness increases with the decrease in the value of dilution. The weld bead having the lowest dilution exhibits the highest microhardness. The observed differences in microhardness with varying degrees of dilution are primarily caused by the increased admixture of base metal elements into the clad bead. At higher dilution levels, enhanced mixing between the substrate and deposited material alters the chemical composition and microstructure of the bead, thereby affecting its microhardness. The fusion zone hardness remains relatively uniform from upper to lower regions, with slightly higher values at the top, which is attributed to a faster cooling rate that promotes finer grain formation. The Heat Affected Zone (HAZ) exhibits higher hardness compared to the base metal, which is due to the growth of grains and alterations in carbon content towards the base metal.

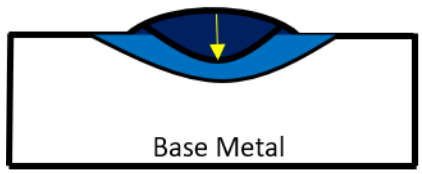

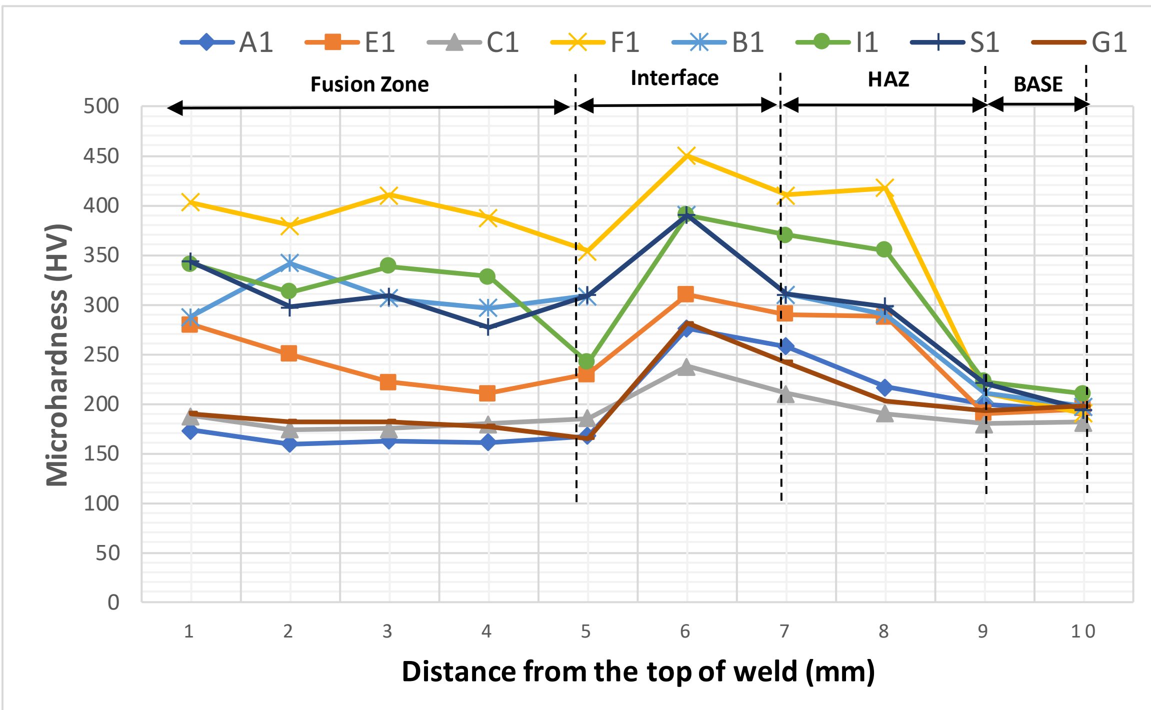

Figure 10. Microhardness of weld bead profiles.

6. Conclusions

The study is focused on the characterization of weld deposits of AISI SS 316L on AISI 1020 steels by hot wire addition in GTAW and robotic weaving technique, to enhance the base metal functionality by reducing the number of passes and richness of admixture of cladding material. The results of these cladding experiments lead to the following outcomes.

- It has been observed that the weld bead penetration and base metal dilution are reduced with an increase in hot wire current. This trend is limited to a hot wire current of the order of 55 A; afterwards, it shows an increasing trend. The weld bead width also increases with hot wire current, accompanied by weaving up to 55 A.
- Base metal dilution has also been reduced from 50 % to 15.96 % when a hot wire with robotic weaving is used for cladding of SS 316 L deposits.

- By employing robotic weaving with hot wire GTAW, microhardness of the order of 450 HV has been recorded in the case of sample F1. Whereas the microhardness was limited to 250 HV in the case of sample C1. This is evident from **Figures 8**, **9**, and **10**, which show different grain-boundary developments in these samples at different dilution values.

Weld beads obtained from weaving and hot-wire GTAW processes, with adequate current and wire-feed settings, exhibit higher microhardness and sufficient dilution. To meet the industrial requirements, the advancement in present processes must be done through: (i) X- ray diffraction analysis must be conducted to get micro-strain and dislocation density values that support the increment in microhardness and a lower value of dilution. (ii) Pulse GTAW process will be the next upgrade with hot wire and weaving technologies to get a stronger path towards the best metallurgical properties to meet modern engineering and marine demands.

Conflicts of Interest
All authors have no conflicts or financial ties with any organization.

Acknowledgments
Funding declaration: This research received no specific grant from any funding agency in the public, commercial, or non-profit sectors. Author contribution declaration (i) Ishank: Conceptualisation (Lead), methodology (Lead), investigation (Lead), writing original draft (equal). (ii) Dr. Jaspal Singh Gill: Formal analysis (Lead), visualisation (Equal). (ii) Dr. Mohd Majid: Supervision (Lead), metallurgical analysis (Equal).

AI Disclosure
The author(s) declare that no assistance is taken from generative AI to write this article.

References

Aloraier, A., Ikpe, A.E., Aladwani, H., & Almashmoum, E. (2025). Analysis of the combined effects of preheating and welding wire feed rates on the FCAW bead geometric characteristics of 1020 steel using fuzzy logic-based prediction models. *Journal of the Mechanical Behavior of Materials*, *34*(1), 20250067. https://doi.org/10.1515/jmbm-2025-0067

Aslam, M., & Sahoo, C.K. (2022). Numerical and experimental investigation for the cladding of AISI 304 stainless steel on mild steel substrate using gas metal arc welding. *CIRP Journal of Manufacturing Science and Technology*, *37*, 378-387. https://doi.org/10.1016/j.cirpj.2022.02.017

Cao, F., Chen, S., & Du, C. (2018). Investigation of hot-wire TIG welding based on the heat-conduction. *Energy Procedia*, *144*, 9-15. https://doi.org/10.1016/j.egypro.2018.06.003

Carvalho, G.H.S.F.L., Venturini, G., Campatelli, G., & Galvanetto, E. (2023). Development of optimal deposition strategies for cladding of Inconel 625 on carbon steel using wire arc additive manufacturing. *Surface and Coatings Technology*, *453*, 129128. https://doi.org/10.1016/j.surfcoat.2022.129128

Chen, Y., He, Y., Chen, H., Zhang, H., & Chen, S. (2014). Effect of weave frequency and amplitude on temperature field in weaving welding process. *The International Journal of Advanced Manufacturing Technology*, *75*(5), 803-813. https://doi.org/10.1007/s00170-014-6157-0

Costa, J.F.M., Jorge, J.C.F., de Souza, L.F.G., Mendes, M.C., Farneze, H.N., & Magalhães, H.A.Y. (2024). Microstructural evaluation of Inconel 625 weld cladding deposited by the GMAW and GMAW with rotating electrode processes. *Technology in Metallurgy, Materials and Mining*, *21*, e2848. https://doi.org/10.4322/2176-1523.20242848 de Oliveira, C.C., Pereira, M., da Silveira, C.A., Dutra, M.K., & Amaral, C. (2023). Effect of wobble parameters on microwelding bead formation of AISI 316L stainless steel. *Journal of Laser Applications*, *35*(4), 042025. https://doi.org/10.2351/7.0001123

Gill, J.S., & Majid, M. (2023). Hot filler wire addition in computer assisted arc welding and cladding processes-a review. In *2023 10th International Conference on Computing for Sustainable Global Development* (pp. 328-332). IEEE. New Delhi, India.

Gill, J.S., & Shahi, A.S. (2016). Combined effect of base metal dilution and thermal aging conditions on the corrosion performance of stainless steel claddings. *Indian Journal of Science and Technology*, *9*(32), 1-6. https://doi.org/10.17485/ijst/2016/v9i32/98738

Hori, K., Watanabe, H., Myoga, T., & Kusano, K. (2004). Development of hot wire TIG welding methods using pulsed current to heat filler wire–research on pulse heated hot wire TIG welding processes. *Welding International*, *18*(6), 456-468. https://doi.org/10.1533/wint.2004.3281

Kumar, A.S., Sharma, S.K., & Shukla, A.K. (2024). Microstructural, mechanical, and thermal analysis of SS316L weldment for marine engineering application. *Journal of Materials Engineering and Performance*, *33*(23), 13502-13515. https://doi.org/10.1007/s11665-023-08906-1

Kumar, N.P., & Shanmugam, N.S. (2020). Some studies on nickel based Inconel 625 hard overlays on AISI 316L plate by gas metal arc welding based hardfacing process. *Wear*, *456*, 203394. https://doi.org/10.1016/j.wear.2020.203394

Li, Z., Liu, C., Xu, T., Ji, L., Wang, D., Lu, J., & Fan, H. (2019). Reducing arc heat input and obtaining equiaxed grains by hot-wire method during arc additive manufacturing titanium alloy. *Materials Science and Engineering: A*, *742*, 287-294. https://doi.org/10.1016/j.msea.2018.11.022

Malhotra, D., Shahi, A.S., & Gupta, K. (2021). Effect of GTAW remelting on the corrosion performance of AISI 316L cladding. *Materials and Corrosion*, *72*(1-2), 141-153. https://doi.org/10.1002/maco.202011666

Manz, A.F. (1964). *A. F. Manz*. https://patents.google.com/patent/US3122629A/en

Munro, C., & Chen, J. (2020). Direct comparison of cold metal transfer to laser hot-wire cladding for AISI 4340 structural steel repair. *Science and Technology of Welding and Joining*, *26*(1), 11-19. https://doi.org/10.1080/13621718.2020.1824450

Neelamegam, C., Meenakshisundaram, R., & Muthukumaran, V. (2024). Process parameter optimization of hot-wire TIG welding of 10 mm thick type 316LN stainless steel plates. *Proceedings of the Institution of Mechanical Engineers, Part C: Journal of Mechanical Engineering Science*, *238*(3), 849-862. https://doi.org/10.1177/09544062231175779

Padmanaban, A., Neelakandan, B., & Kandasamy, D. (2017). A study on process characteristics and performance of hot wire gas tungsten arc welding process for high temperature materials. *Materials Research*, *20*(1), 76-87. https://doi.org/10.1590/1980-5373-MR-2016-0321

Pai, A., Sogalad, I., Albert, S.K., Kumar, P., Mitra, T.K., & Basavarajappa, S. (2014). Comparison of microstructure and properties of modified 9Cr-1Mo welds produced by narrow gap hot wire and cold wire gas tungsten arc welding processes. *Procedia Materials Science*, *5*, 1482-1491. https://doi.org/10.1016/j.mspro.2014.07.335

Pavan, A.R., Sakthivel, T., Arivazhagan, B., Vasudevan, M., Ashish, K., & Karthik, V. (2023). A comparative study on the microstructural evolution and mechanical behavior of 316LN stainless steel welds made using hot-wire tungsten inert gas and activated tungsten inert gas process. *Journal of Materials Engineering and Performance*, *33*(23), 13618-13636. https://doi.org/10.1007/s11665-023-08881-7

Raj, P., & Gill, J.S. (2023). Characterisation of weld bead and microhardness of SS316L weld overlays on S355J2+N steel using GTAW under E-type magnet. *Engineering Research Express*, *5*(4), 045039. https://doi.org/10.1088/2631-8695/ad058c

Rashid, R.R., Abaspour, S., Palanisamy, S., Matthews, N., & Dargusch, M.S. (2017). Metallurgical and geometrical characterisation of the 316L stainless steel clad deposited on a mild steel substrate. *Surface and Coatings Technology*, *327*, 174-184. https://doi.org/10.1016/j.surfcoat.2017.08.013

Sandhu, S.S., & Shahi, A.S. (2016). Metallurgical, wear and fatigue performance of Inconel 625 weld claddings. *Journal of Materials Processing Technology*, *233*, 1-8. https://doi.org/10.1016/j.jmatprotec.2016.02.010

Sashank, S.S., Rajakumar, S., & Karthikeyan, R. (2024). Influence of electrode current on mechanical and metallurgical characteristics of hot wire TIG welded SS304HCu austenitic stainless steel and P91 ferritic steel dissimilar joints. *International Journal on Interactive Design and Manufacturing*, *18*(7), 5261-5270. https://doi.org/10.1007/s12008-024-01835-w

Shakya, P., Singh, K., & Arya, H.K. (2024). Influence of dual axial magnetic field and welding parameters on weld characteristics in GTAW process. *Journal of Adhesion Science and Technology*, *40*(3), 567-585. https://doi.org/10.1080/01694243.2024.2385570

Tsuyama, T., Nakai, K., & Tsuji, T. (2014). Development of submerged arc welding method using hot wire. *Welding in the World*, *58*(5), 713-718. https://doi.org/10.1007/s40194-014-0153-8

Wang, X., Hu, Q., Li, T., Liu, W., Tang, D., Hu, Z., & Liu, K. (2022). Microstructure and fracture performance of wire arc additively manufactured Inconel 625 alloy by hot-wire GTAW. *Metals*, *12*(3), 510. https://doi.org/10.3390/met12030510

Zhao, J., Xu, G., Wang, Z., Ju, J., Wang, X., Chen, M., Xue, F., & Zhou, J. (2024). Effect of weaving on Fe3Al layers prepared by arc deposition technique. *Journal of Materials Engineering and Performance*, *33*(2), 706-723. https://doi.org/10.1007/s11665-023-08166-z